Available online at www.sciencedirect.com

ScienceDirect

journal homepage: http://www.elsevier.com/locate/acme

Original Research Article

Investigation on fatigue behaviour of load-carrying fillet welded joints based on mix-mode crack propagation analysis

Liang Zong [a,b,c], *Gang Shi* [c], *Yuan-Qing Wang* [c,*], *Jia-Bao Yan* [a,b], *Yang Ding* [a,b]

[a] *School of Civil Engineering, Tianjin University, Tianjin 300072, PR China*
[b] *Key Laboratory of Coast Civil Engineering Structures Safety, Ministry of Education, Tianjin 300072, PR China*
[c] *Key Laboratory of Civil Engineering Safety and Durability of China Education Ministry, Department of Civil Engineering, Tsinghua University, Beijing 100084, PR China*

ARTICLE INFO

Article history:
Received 21 October 2016
Accepted 29 January 2017
Available online 3 March 2017

Keywords:
Fatigue
Load-carrying fillet weld
3D mix-mode propagation
Initial crack
Fracture mechanics

ABSTRACT

The fatigue behaviour of the load-carrying fillet welded joints was investigated by experimental and numerical approach in this paper. 26 load-carrying cruciform fillet welded joints involving 8 stress levels were tested and the S–N curves of 95% survival probability in terms of toe failure and root failure were established separately. The test results also demonstrate that the design curves of Eurocode3 are not suitable for this batch of specimens. In the following numerical simulations, three types of initial crack assumption were analysed by 3D mix-mode fatigue crack propagation analysis according to experimental observation. All the possible crack growth routes were simulated well. However, the single crack assumptions cannot form satisfactory simulations on fatigue lives with enough safety stock. Therefore, multi-crack analysis was conducted based on the combined data in terms of both toe failure and root failure. It is found that multi-crack analysis with 0.5 mm weld toe initial line crack and 0.1 mm weld root initial line crack can provide appropriate prediction. The findings can be beneficial for the fatigue assessment of load-carrying fillet welded joints fabricated by the normal welding technique in China and offer some references for the fatigue assessment of structural details with different possible failure modes.

1. Introduction

Load-carrying fillet welded joint (LCFWJ) is one of the most typical fatigue prone structural details. Many efforts have been made to investigate its fatigue behaviour [1]. The most direct approach is the experimental observations and extensive fatigue tests on LCFWJ have been conducted [2,3]. On the basis of the numerous test data, reliable S–N curves were established and adopted in many design codes, such as BS5400 [4], Eurocode3 [5] and AASHTO [6]. Meanwhile, more and more refined fatigue assessment approaches have been developed,

* *Corresponding author at*: Department of Civil Engineering, Tsinghua University, Beijing 100084, PR China. Fax: +86 10 6278 2708.
E-mail address: wang-yq@tsinghua.edu.cn (Y.-Q. Wang).

http://dx.doi.org/10.1016/j.acme.2017.01.009

which can be classified into two types. One is the 'stress-life' approach, including the hot spot stress (HSS) approach [7,8] and effective notch stress approach [9,10], the other one is the Fracture Mechanics based approach [11,12]. All the 'stress-life' approaches depend on appropriate design curves, which can only be established by fatigue tests. For structural details made by new materials, new welding techniques or even new weld shapes, the applicability of the existing design curves is limited and fatigue tests have to be conducted in most cases, which are quite time and money consuming. From the view of Fracture Mechanics, fatigue failure is the process of the fatigue crack initiation and propagation. Due to the inevitable defects in fillet welds, the propagation life can be regarded as the total fatigue life. This approach only requires appropriate fatigue crack growth model of the corresponding materials [13,14], which costs much less than the fatigue tests on different types of structural details. Many researches based on Fracture Mechanics have been conducted on the LCFWJ [15]. Nevertheless, the existing work was mainly carried out on the basis of planar model and mode I type crack assumption, which has relevant analytical solutions for stress intensity factor (SIF) of the crack front. However, fatigue cracks in practical structures usually belong to mix-mode cracks due to the complexity of loading and local geometry. Even the initial cracks belongs to mode I type, they will probably become mix-mode cracks after a period of propagation. Therefore, the mix-mode crack propagation analysis is of great importance to reveal the more actual fatigue behaviour of key structural details.

In this paper, the fatigue behaviour of LCFWJ was investigated based on both fatigue tests and 3D mix-mode fatigue crack propagation analysis. The experimental *S–N* curve of 95% survival probability was established, which can replenish the public fatigue database in China. Three initial crack assumptions were analysed and the corresponding fatigue performance was discussed in details. According to the comparison between the predicted and the experimental fatigue lives, the most suitable initial crack assumption was recommended for LCFWJ in terms of the steel materials and the normal welding technique in China.

2. Experimental investigation

2.1. Specimen preparation

Cruciform specimens of LCFWJ were adopted in the fatigue test. Fig. 1 shows the geometric scheme of the specimens. The fillet weld foot was designed to be 8 mm. The steel plates were welded by MCAW with 240 ± 20 A welding current and 30 ± 2 V welding voltage. Two panels were fabricated in ZiJingGuan Bridge Plant, which is a typical bridge construction company and could represent the mean level of bridge construction technique in China. Each panel was cut up into 13 specimens by mechanical processing, each 50 mm wide. All the steel plates belong to Q345qD grade, which are in the exactly same batch with that in Ref. [14] for fatigue crack growth rate tests. Therefore, the coupon test result and fatigue crack growth rate test data in [14] can be applied in the following numerical analysis of this paper.

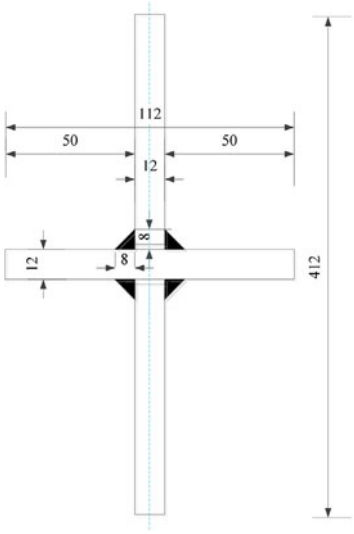

Fig. 1 – Geometric scheme of test specimens.

2.2. Experimental programme

Constant amplitude fatigue tests were implemented by PLG-200C fatigue test machine of ±10 t loading capacity. The loading frequency depends on the stiffness of the specimens. It would decrease if the stiffness of the specimen decreases, which represents certain extent fatigue damage occurred in the specimen. The maximum fatigue life was settled as 5 million cycles. The test would stop when the loading frequency had a 10 Hz drop or the loading cycles reached up to 5 million cycles.

The stress ratio for the test was 0.1. According to Eurocode3 [5], the cruciform joints with fillet welds are classified as FAT63 and FAT36 with respect to weld toe failure and weld root failure, respectively. The nominal stress range for weld toe is just the stress range in the vertical plate, $\Delta\sigma$, as shown in Fig. 2. The nominal stress range for weld root failure is the stress range in the fillet welds and the related calculation approach is specified in Eurocode3. The minimum $\Delta\sigma$ was determined to be 54 MPa (the corresponding nominal stress range at the weld root is about 48 MPa), which is between FAT63 and FAT36. The maximum tensile stress kept increasing at a 10 MPa interval in the following tests until eight stress levels were involved in the whole test. Therefore, the maximum stress was taken from 60 MPa to 130 MPa. The loading cases were numbered by NFW1 to NFW8, accordingly. The geometric profile of the specimens would be measured as shown in Fig. 2, which can provide modelling data for the following numerical simulation.

3. Experimental observations

3.1. Geometric measurement

To obtain the accurate geometric profile of the joints, the thickness of the main plates was measured in the first step. The average value of t_1 and t_2 is 11.85 mm and 11.83 mm, respectively. Based on the thickness of the steel plates, the

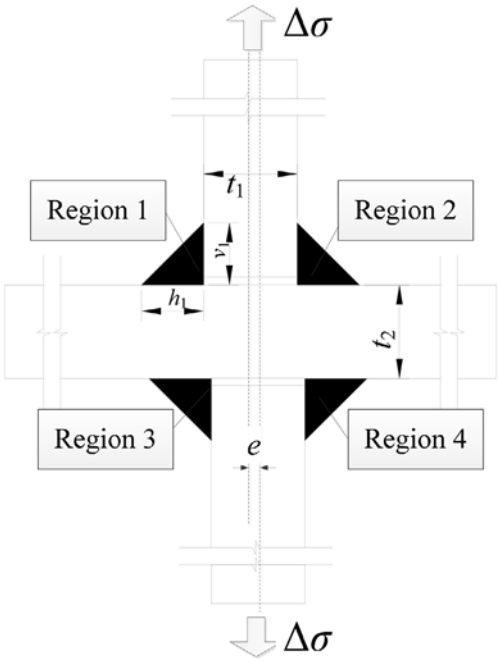

Fig. 2 – Geometric profile measurement.

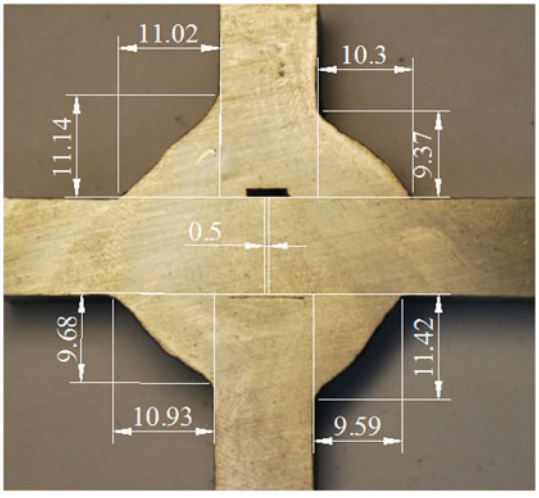

Fig. 3 – Geometric measurement on test specimens.

detailed profile of fillet welds could be depicted using its high-quality image. Fig. 3 presents a typical geometric profile image, which can be measured by importing into AutoCAD software. The average measured dimensions were recorded in Table 1.

The design value of h and v for all the welds is 8 mm and the average weld dimension is 1.45–1.89 mm larger than that of the designed weld, which meets the demands of Chinese code GB50661 [15].

3.2. *Fatigue test results*

26 specimens were tested in total and all the effective data is recorded in Table 2. Half the specimens fail at the weld toes and half the specimens fail at the weld roots. The weld toe failure mode involves two patterns. One pattern is that line crack occurred along the specimen width (see Fig. 4(a)) and the other one is that crack only develops in part of the specimen (see Fig. 4(b)). For the weld toe failure mode, the fatigue crack propagated through about half of the plate from the side view. For the weld root failure mode, line crack pattern always occurred (see Fig. 4(c)) and the fatigue crack propagated through about 80% thickness of the welds. Weld toe failure and root failure did not occur in the same specimen.

All the effective data was plotted in the logarithmic coordinate system, as shown in Fig. 5. Due to the difference between weld toe failure and weld root failure, the corresponding test data were analysed separately using linear fitting approach. As the test data are not sufficient and evenly distributed to determine m, the slope of S–N curve ($\log N + m \log S = C$), a fixed value of $m = 3$ was taken according to the recommendations of IIW [8]. Then the lower bound of the test data of 95% survival probability was derived, as shown in Fig. 5. The design S–N curves of Eurocode3 for LCFWJ were also presented. It is found that the fatigue strength related to root failure is higher than that related to toe failure. The fitting curve for toe failure and root failure is about FAT56 and FAT47, respectively. The corresponding lower bound of 95% survival probability is FAT37 and FAT26 respectively, which is obviously under the design S–N curves, FAT63 and FAT36, specified in Eurocode3. It is possibly connected with the quality of manual welding. On all accounts, it is proved that the design curves of Eurocode3 are not suitable for this batch of specimens and the test data could provide useful reference for making suitable S–N curves for LCFWJ fabricated in China. In fact, the welding quality control principle is similar with GB50661 in most design codes, such as EN ISO 1090-2 [16] and AWS D1.1 [17], while, in which penetration testing or magnetic particle testing is recommended. Although these two techniques can only detect the surface flaws, they can guarantee a better welding quality of the joints. Furthermore, from the view of the whole welding process, the quality control in industrial developed countries is more strict and reliable. It is probably the reason that Eurocode3 is not suitable for the specimen batch used in research.

Table 1 – Measured average dimensions.

Item (mm)	t_1	t_2	e	Region 1		Region 2		Region 3		Region 4	
				h_1	v_1	h_2	v_2	h_3	v_3	h_4	v_4
Averaged measurement	11.85	11.83	1.96	9.57	9.58	9.45	9.45	9.89	9.76	9.79	9.84

Table 2 – Fatigue test results.

No.	σ_{max} (MPa)	Failure pattern	Fatigue life (cycle)	No.	σ_{max} (MPa)	Failure pattern	Fatigue life (cycle)
LFW1-1	130	Weld toe failure	214500	LFW5-2	90	Weld toe failure	608738
LFW1-2	130	Weld root failure	612100	LFW5-3	90	Weld toe failure	538695
LFW1-3	130	Weld root failure	206234	LFW6-1	80	Weld root failure	256961
LFW2-1	120	Weld toe failure	602991	LFW6-2	80	Weld toe failure	328896
LFW2-2	120	Weld toe failure	460568	LFW6-3	80	Weld root failure	294796
LFW2-3	120	Weld toe failure	323194	LFW6-4	80	Weld toe failure	810030
LFW2-4	120	Weld root failure	343144	LFW6-5	80	Weld toe failure	552986
LFW3-1	110	Weld root failure	482628	LFW7-1	70	Weld toe failure	962772
LFW3-2	110	Weld toe failure	523176	LFW7-3	70	Weld toe failure	1488320
LFW3-3	110	Weld toe failure	602503	LFW7-3	70	Weld root failure	1088900
LFW4-1	100	Weld root failure	548100	LFW0-1	60	Weld root failure	677008
LFW4-2	100	Weld root failure	674549	LFW0-2	60	Weld root failure	2296250
LFW5-1	90	Weld root failure	632400	LFW0-3	60	Weld root failure	2085860

Note: σ_{max} is the maximum stress applied in the vertical plate.

(a) Weld toe failure of through crack pattern (b) Weld toe failure of non-through crack pattern (c) Weld root failure

Fig. 4 – Failure mode.

4. Mix-mode crack propagation analysis

4.1. *Quasi-static propagation analysis theory*

Quasi-static propagation analysis requires a discretization of the whole crack propagation procedure and conducts static analysis on the corresponding numerical models at different crack sizes [18,19]. With the help of this approach, the approximate relationship between crack size and SIF range (a–ΔK relationship) can be simulated, and then the predicted fatigue life can be calculated by adopting an appropriate crack growth model. The following four items will directly determine the effectiveness of quasi-static propagation analysis for mix-mode fatigue cracks.

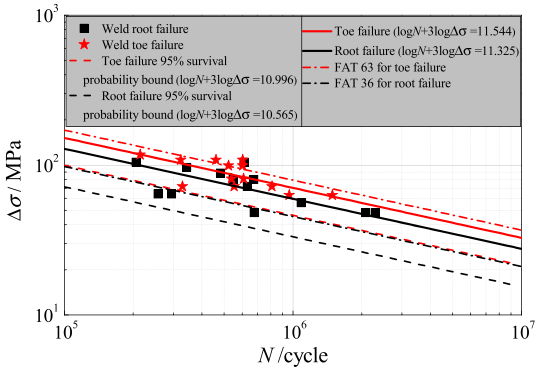

Fig. 5 – Fatigue test results.

(1) Appropriate fatigue crack growth model should be determined. There have been several formulas for describing the fatigue crack growth principle, among which Paris Law [20] is the most distinguished and concise choice. Therefore, Paris Law is adopted in this paper and the corresponding parameters for the steel plates of this batch have been identified by the authors [14]. For weld toe failure mode, the parameters are taken as $\log C = -10.82$ and $m = 2.66$ in terms of the 'N, mm' unit system. For weld root failure, $\log C = -10.86$ and $m = 2.67$ were used in terms of the same unit system. For mix-mode fatigue cracks, the effective SIF range ΔK_{eff} proposed by Tanaka [21] (Eq. (1)) was adopted in this paper:

$$\Delta K_{eff} = \sqrt[4]{\Delta K_I^4 + 8\Delta K_{II}^4} \tag{1}$$

where ΔK_I and ΔK_{II} is the SIF range in terms of mode I and mode II, respectively. Then, the fatigue crack propagation rate (da/dN) is given according to the Paris Law by

$$\frac{da}{dN} = C(\Delta K_{eff})^m \tag{2}$$

The predicted fatigue life N can be given by

$$N = \int_{a_0}^{a_{cr}} \frac{da}{C(\Delta K_{eff})^m} = \int_{a_0}^{a_{cr}} \frac{da}{C(f(a))^m} \tag{3}$$

where a_0 is the initial crack length and a_{cr} is the critical crack length. It can be easily found that the predicted fatigue life can be obtained based on the integration of the accurate a–ΔK relationship, i.e., $f(a)$ in Eq. (3).

(2) Determination of crack propagation direction, i.e., kink angle. Kink angle has a great influence on the computed SIF. The mix-mode fatigue crack usually will not grow in its original crack plane due to the presence of mode II condition. There are several criteria to determine the king angle, which are always aimed to reduce the SIF related to mode II condition, including the maximum tensile stress criterion (MTS) [22], the maximum generalized stress criterion (GEN) [23], and the maximum strain energy release rate criterion (SERR) [24]. MTS is adopted in the following analysis because it is the most recognized criteria. The computed kink angle θ according to MTS criteria is given by

$$\theta = \cos^{-1}\left\{\frac{3K_{II}^2 + K_I\sqrt{K_I^2 + 8K_{II}^2}}{K_I^2 + 9K_{II}^2}\right\} \tag{4}$$

(3) Determination of the crack increment Δa of each step. For the simulation of the load-carrying fillet welded specimens herein, the crack increment of the front point in terms of the median ΔK value, i.e., Δa_{median} is set to be 0.1 mm. The other front points' increment can be given by [25]

$$\Delta a_i = \Delta a_{median}\left(\frac{\Delta K_i}{\Delta K_{median}}\right)^m \tag{5}$$

where Δa_i and ΔK_i are the crack extension and SIF range of the ith crack front point, respectively. m is taken as 2.66 and 2.67 for weld toe failure mode and weld root failure mode, respectively. With the help of Eq. (4), the new crack front can be obtained.

(4) Establishment and update of FE model with high-quality crack front mesh. The advanced adaptive remesh technique should be adopted to meet this demand. In this paper, the combined analysis platform of Franc3D [25] and Abaqus is adopted, in which Franc3D is in charge of remeshing the model and Abaqus is used as a solver to calculate the mechanical response of the cracked model.

4.2. *Determination of initial cracks and corresponding analytical models*

Initial crack has a great effect on the predicted fatigue life. On the basis of the experimental phenomenon, three types of initial cracks were considered. In terms of the specimens failed at the weld toes in the pattern of through crack, the I-type line initial crack was assumed, as shown in Fig. 7(a). The numerical model can be simplified as a planar model and its analytical solution of the SIF can be given by

$$\Delta K = \Delta\sigma\cdot\sqrt{\pi a}\cdot v\left(\frac{a}{B}\right)^w\left[1.12-0.38\left(\frac{a}{B}\right)+10.6\left(\frac{a}{B}\right)^2-21.7\left(\frac{a}{B}\right)^3 + 30.4\left(\frac{a}{B}\right)^4\right] \tag{6}$$

The definitions of the geometries a and B are shown in Fig. 7 (a). The values of v and w are functions of L/B, which is specified in Table M.9 in [28]. The presence of obvious axial alignment should not be ignored, which can cause an increase or decrease in stress at the joint due to the introduction of local bending stresses. The effect of misalignment can be expressed in terms of the maximum factor by which the applied nominal stress is magnified as a result of its presence. The magnification factor for fillet welded joints is given by [28]

$$k = \frac{\kappa e l_1}{B(l_1 + l_2)} + 1 \tag{7}$$

The definitions of the geometries e, B, l_1 and l_2 are shown in Fig. 6. Based on the boundary conditions in the test, κ is taken as 6.75 [28]. For the specimens of this batch, the magnification factor is 1.55 according to Eq. (7).

As for the specimens failed at the weld toes in the pattern of non-through crack, the semi-elliptical initial crack is assumed, as shown in Fig. 7(b). The value of a/c is taken as 1/4 according to [29]. The frequently-used analytical solution for SIF of such crack is the empirical solution proposed by Newman and Raju (Eq. (8)):

$$K = (M_{kt}\sigma_t + M_{kb}\sigma_b)f_w\frac{\sqrt{\pi a}}{Q} \tag{8}$$

where σ_t and σ_b are nominal tensile stress and bending stress; M_{kt} and M_{kb} are the stress magnification factor in terms of tension and bending; f_w is the finite width correction factor; Q is the complete elliptic integral of the second kind. However, for semi-elliptical cracks in local welds, there is no precise analytical solutions for such details and it is usual to modify Eq. (8) by the magnification factor specified by BS7910. Therefore, the analytical solution for this initial crack assumption will not discussed in the following analysis.

Based on the observations on the specimens failed at weld root, another possible assumption is that the initial crack occurred at the weld roots as a line crack (see Fig. 7(c)). The corresponding analytical solution is given by

$$K = M_k f_W \sigma\sqrt{\pi a_w} = M_k f_W \sigma\sqrt{\pi\left(a + \frac{B}{2}\right)} \tag{9}$$

where M_k is the stress magnification factor; σ is the nominal tensile stress; a is the crack size. The presence of axial misalignment will also affect the stress distribution around the weld root. The magnification factor for the weld throat k can be given by [28]

$$k = \frac{\kappa e l_1}{B(l_1 + l_2)}\cdot\frac{e}{B + h_f} + 1 \tag{10}$$

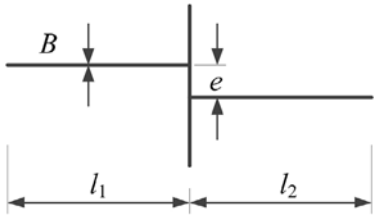

Fig. 6 – Schematic diagram of axial alignment.

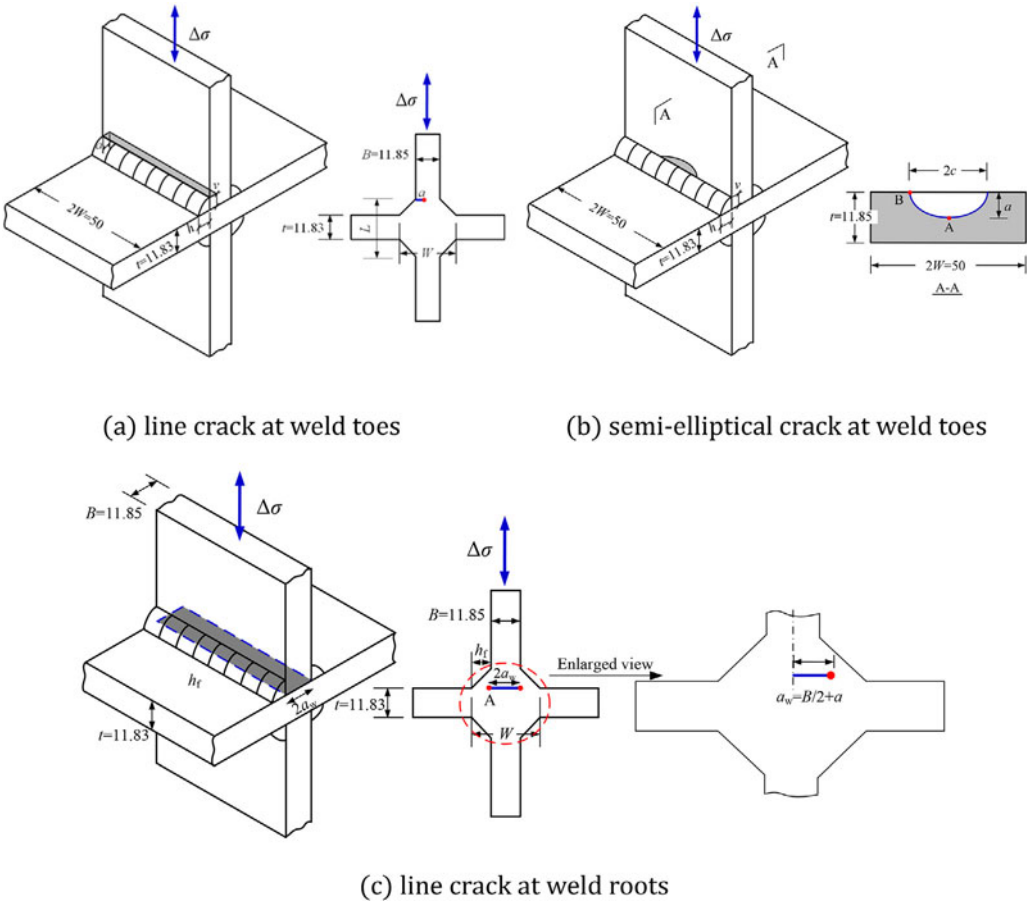

Fig. 7 – Determination of initial crack.

The definitions of the geometries e, B, l_1 and l_2 are in line with Eq. (7) and h_f is shown in Fig. 7(c). For the specimens of this batch, the magnification factor in terms of misalignment is 1.05, which means the presence of axial misalignment has little influence on the applied stress. In the following analysis, the depth for all the initial crack types (the value of a) is assumed to be 0.3 mm according to previous studies [15].

4.3. *Discussion and recommendation*

(1) Comparisons between numerical and analytical solutions. As mentioned before, accurate fatigue life prediction depends on accurate a–K relationship. Therefore, the SIF solutions derived by numerical and analytical approaches are compared with each other as shown in Figs. 8 and 9. For the line crack at weld toes, the numerical solutions are generally in line with

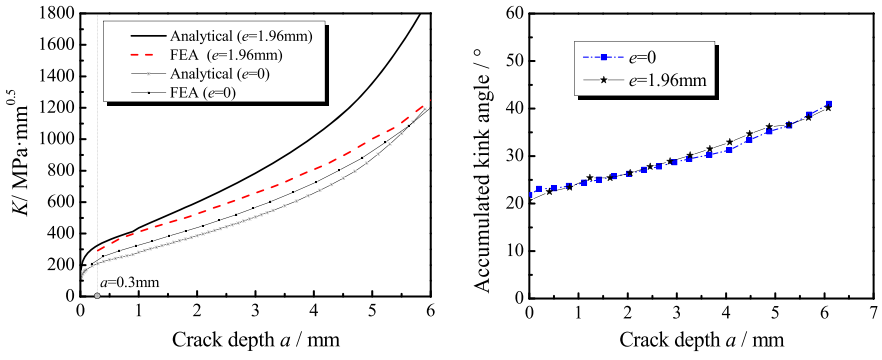

(a) a-K relationship (b) kink angle

Fig. 8 – Comparison of K derived by numerical and analytical approaches for line crack at weld toes.

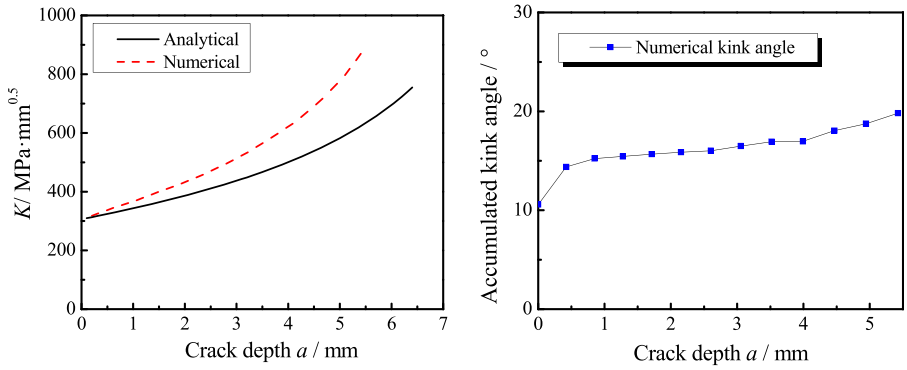

(a) a-K relationship (b) kink angle

Fig. 9 – Comparison of K derived by numerical and analytical approaches for line crack at weld roots.

the analytical solutions when axial misalignment is not considered (see Fig. 8a). However, the difference will increase when the axial misalignment is considered and it will be enlarged with the crack growth. This is because the presence of line crack will serve to reduce local bending stresses resulting from misalignment.

The accumulated kink angle development with the increase of the crack depth is presented in Fig. 8(b). It can be found that the actual fatigue crack will show up obvious mix-mode behaviour as the kink angle is larger 20°. Therefore, the fatigue crack cannot be regarded as I type mode during the whole crack development process and mix-mode crack analysis is necessary.

As for the line crack at weld roots, the a–K relationships based on the actual model of 1.96 m are presented. It is found that the analytical solutions are in complete agreement with the numerical solutions at the very initial period, which proves the rationality of the FEA. However, the difference will increase between the analytical and the numerical solutions due to the crack kink effect (see Fig. 9(a)). The accumulated kink angles is presented in Fig. 9(b), which proves the mix-mode crack analysis is necessary once again.

(2) Suitable initial crack assumption. The predicted fatigue life computed by quasi-static propagation analysis based on different initial crack assumptions are shown in Fig. 10. The average ratio of experimental fatigue lives over predicted fatigue lives, denoted by η, and the fatigue strength in terms of 2 million fatigue loading cycles, denoted by FAT, are derived and recorded in Table 3, where η is given by

$$\eta = \frac{(\sum_{i=1}^{n} N_{test,i}/N_{FE,i})}{n} \tag{11}$$

where $N_{test,i}$ and $N_{FE,i}$ is the experimental and numerical fatigue life of the ith specimen. n is the total number of the specimens.

It is obvious that the semi-elliptical crack assumption provides extensively longer fatigue lives than the experimental fatigue lives and thus to be inappropriate. The predicted fatigue lives are much more acceptable based on the initial line crack assumption at weld toes or roots. In terms of the assumption that line crack develops at weld toes, η is 2.12, which seems to give a relatively accurate prediction on fatigue lives of the specimens. However, the predicted fatigue lives still do not have enough safety stock as the discreteness of test data is really significant. The same situation happens for the assumption that line crack develops at the weld root. The corresponding η is 1.42. Nevertheless, the safety stock is still not sufficient in comparison with the lower bound S–N curve.

To propose an appropriate initial crack assumption for LCFWJ, parametric analysis in terms of initial crack size was conducted. The initial crack size was taken as 0.3 mm, 0.4 mm and 0.5 mm for both toe crack model and root crack model, respectively. The predicted S–N curves are shown in Fig. 11. It can be easily found that the predicted fatigue lives get closer to

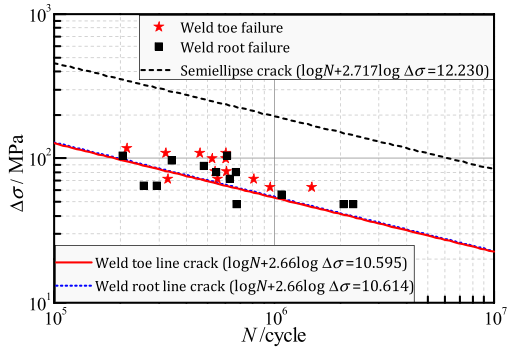

Fig. 10 – The predicted fatigue life based on different initial crack assumptions.

Table 3 – Comparison of all the predicted results based on different assumptions.

Assumed condition	η	FAT (MPa)
Semi-elliptical crack at weld toe	0.06	152.0
Line crack at weld toe	2.12	41.1
Line crack at weld root	1.42	41.8
95% survival probability bound for toe failure	3.91	36.7
95% survival probability bound for root failure	6.96	26.4

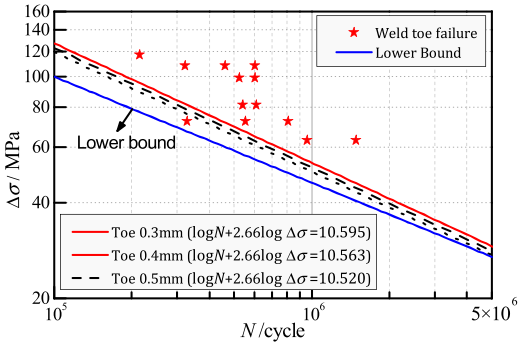

(a) Weld toe failure

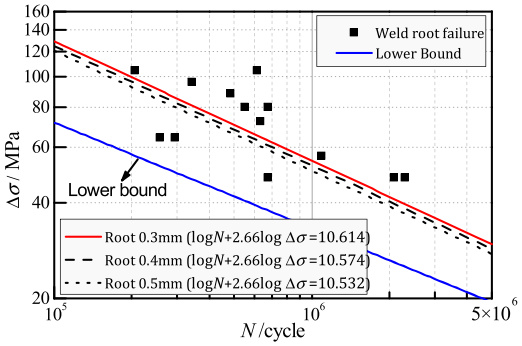

(b) Weld root failure

Fig. 11 – The predicted fatigue life based on different initial crack sizes.

the lower bound *S–N* curves of the test specimens as the initial crack size increases. When the crack size is 0.5 mm, η is 2.52 for toe crack model and 1.71 for root crack model, which is less than that derived according to the lower bound curve, especially for the root crack model. It is proved the safety stock is still not enough, which mainly due to the significant discreetness of the test results. Therefore, continued discussion should be conducted on the safety stock in the following section.

In addition to the predicted fatigue lives, the predicted fatigue crack propagation routes are compared with that recorded by experimental observations, as shown in Fig. 12. It is found that the predicted and observed crack growth routes are properly in line with each other, which means the crack kink effect is well considered and proves the reasonability of the mix-mode crack growth analysis.

(3) Multi-crack propagation analysis. Crack-like defects probably exist in many locations of a fillet welded joints. The above discussions mainly focus on the development of one crack at weld toes or weld roots, on the basis of weld toe failure mode or weld root failure mode observed in the fatigue tests. Despite no obvious failure occurred at both locations, this does not mean that crack-like defect only exist at the location where failure occurred. The crack-like defects at other locations may not develop very seriously and thus to be invisible, but they would probably affect the stress distribution of the joints and then affect the development of the main crack. Furthermore, the safety stock calculated based on the single crack assumption is not enough. Therefore, it is meaningful to conduct multi-crack analysis for LCFWJ. Nevertheless, there are two issues that should be well settled. The first is that which nominal stress should be used when multi-crack analysis is conducted? Herein we use the nominal stress in terms of weld toe failure, which is a direct indicator for the applied tensile load. All the fatigue test results related to the two failure modes are combined and depicted using the same definition of nominal stress. The second issue is that how to determine the combinations of the defects. A typical situation which

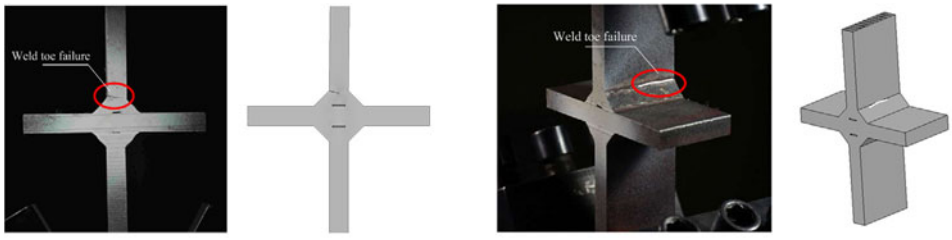

(a) Weld toe failure of through crack pattern (b) Weld toe failure of non-through crack pattern

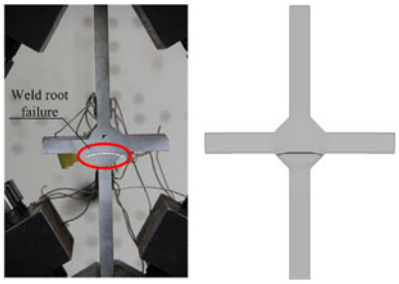

(c) Weld root failure

Fig. 12 – The predicted and observed crack growth routes.

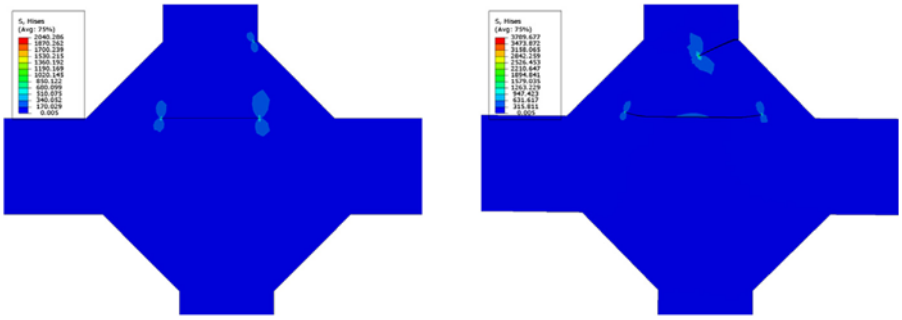

(a) FE model with initial crack (b) FE model with critical crack

Fig. 13 – The multi-crack analysis model.

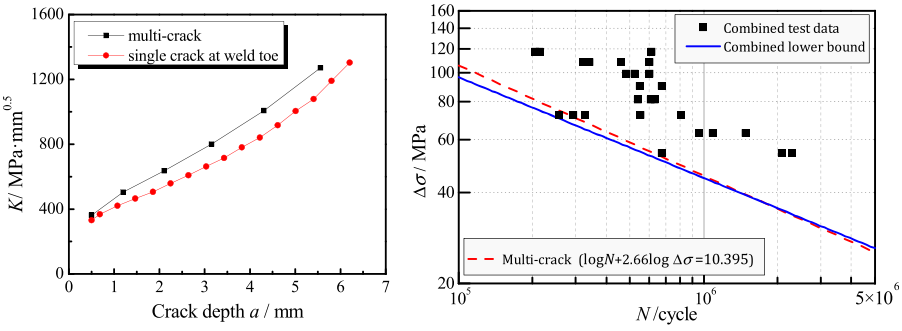

(a) *a*-*K* relationship (b) predicted S-N curve

Fig. 14 – The multi-crack analysis results.

contains both weld toe crack and weld root crack is chosen herein (see Fig. 13). Because the nominal stress in terms of weld toe failure is used, the initial crack at weld toe is regarded as the main crack and its initial depth is taken as 0.5 mm. The crack at weld root is regarded as secondary crack and its depth is taken as 0.1 mm. All the initial cracks are assumed as line cracks. Fig. 14 shows the predicted *a*–*K* relationship and *S*–*N* curve. In comparison with the *a*–*K* relationship based on the single weld toe crack model, it is found that the SIF is enlarged due to the presence of the weld root crack. Meanwhile, the simulated *S*–*N* curve can cover all the test data and also be closer to the lower bound *S*–*N* curve for the combined test data. It can be concluded that multi-crack analysis tends to provide more appropriate predictions for the test in this paper. As for the load-carrying fillet welded joints, it is recommended to conduct multi-crack propagation analysis based on the FE model shown in Fig. 13(a) according to its good prediction on the specimens of this batch.

5. Conclusions

The fatigue performance of LCFWJ has been investigated in this paper. Fatigue tests were conducted on 26 specimens and 3D mix-mode fatigue crack growth simulation was developed based on three initial crack assumptions. Comparison between the predicted and experimental fatigue lives was carried out. Key conclusions and suggestions can be drawn:

(1) Experimental S-N curves and their lower bounds of 95% survival probability for LCFWJ in terms of two failure modes were established based on 26 effective fatigue test data involving 8 stress levels. The experimental *S*–*N* curves are representative on reflecting the fatigue performance of the load-carrying fillet welded details fabricated in China and can provide useful references for the related design codes. It is also demonstrated that the design curves of Eurocode3 are not suitable for this batch of specimens.

(2) Both weld toe failure mode and weld root failure mode occurred during the fatigue tests, and three types of initial crack assumption were analysed by the 3D mix-mode fatigue crack propagation analysis according to the experimental observation. All the possible crack growth routes can be simulated well. In terms of the predicted fatigue lives of the specimens, it is proved that multi-crack analysis with 0.5 mm weld toe initial line crack and 0.1 mm weld root initial line crack can provide the most appropriate prediction.

(3) The fatigue test results related to weld toe failure and weld root failure are combined using a same definition of nominal stress in the multi-crack analysis, based on which

the appropriate initial crack assumption is obtained. The findings are suitable for this batch of specimens and LCFWJ with similar geometric profiles. However, it still needs further verification to determine whether the findings are suitable for LCFWJ of quite different geometric profiles, such as thicker plates, larger weld legs and so on. On all accounts, the research work provides a basic assessment approach in terms of the combined test data of toe failure and root failure and can offer references for the fatigue assessment of structural details with various failure modes .

Acknowledgements

The authors gratefully acknowledge the support for this work, which was sponsored by the National Natural Science Foundation of China (Nos. 51678339 and 51608359) and the Project funded by China Postdoctoral Science Foundation (Nos. 2015M581300 and 2016T90206). The kind support on the permission to use Franc3D from Mr. Li Mengguang in MVT GROUP INC. is also greatly appreciated.

REFERENCES

[1] K.J. Kirkhope, R. Bell, L. Caron, et al., Weld detail fatigue life improvement techniques. Part 1. Review, Marine Structures 12 (6) (1999) 447–474.
[2] S.J. Maddox, Hot-spot stress design curves for fatigue assessment of welded structures, International Journal of Offshore and Polar Engineering 12 (2) (2002) 134–141.
[3] S. Kainuma, T. Mori, A fatigue strength evaluation method for load-carrying fillet welded cruciform joints, International Journal of Fatigue 28 (8) (2006) 864–872.
[4] British Standards Institution (BSI), BS 5400. Steel, Concrete and Composite Bridges – Part 10: Code of Practice for Fatigue, BSI, London, 1980.
[5] European Committee for Standardization (CEN), EN 1993-1-9 Eurocode 3. Design of Steel Structures – Part 1–9: Fatigue, CEN, Brussels, 2005.
[6] American Association of State Highway and Transportation Officials (AASHTO), LRFD Bridge Design Specifications, 3rd ed., AASHTO, Washington, DC, 2004.
[7] F.Z. Akhlaghi, Fatigue Life Assessment of Welded Bridge Details Using Structural Hot Spot Stress Method: A Numerical and Experimental Case Study, (Master's thesis), Chalmers University of Technology, Göteborg, Sweden, 2009.
[8] A.F. Hobbacher, The new IIW recommendations for fatigue assessment of welded joints and components – a comprehensive code recently updated, International Journal of Fatigue 31 (1) (2009) 50–58.
[9] D. Radaj, C.M. Sonsino, W. Fricke, Fatigue Assessment of Welded Joints by Local Approaches, Woodhead Publishing Ltd., Cambridge, 2006.
[10] D. Radaj, Design and Analysis of Fatigue Resistant Welded Structures, Woodhead Publishing Ltd., Cambridge, 1990.
[11] X.W. Ye, Y.H. Su, J.P. Han, A state-of-the-art review on fatigue life assessment of steel bridges, Mathematical Problems in Engineering 2014 (2014) 1–13.
[12] J.W. Fisher, K.H. Frank, M.A. Hirt, et al., NCHRP Report 102: Effect of Weldments on the Fatigue Strength of Steel Beams, Transportation Research Board, National Research Council, 1970.
[13] L. Zong, G. Shi, Y. Wang, Experimental investigation and numerical simulation on fatigue crack behavior of bridge steel WNQ570 base metal and butt weld, Construction and Building Materials 77 (2015) 419–429.
[14] L. Zong, G. Shi, Y. Wang, Experimental investigation on fatigue crack behavior of bridge steel Q345qD base metal and butt weld, Materials & Design 66 (2015) 196–208.
[15] Z. Barsoum, Residual Stress Analysis and Fatigue Assessment of Welded Steel Structures, (Ph.D. dissertation), Royal Institute of Technology (KTH), Stockholm, Sweden, 2008.
[16] EN B.S. 1090-2, Execution of Steel Structures and Aluminum Structures – Part 2: 2. Technical Requirements for the Execution of Steel Structures, British Standards Institution, London, 2008.
[17] AWS D.1/D1.1M, 2008 Structural Welding Code-Steel, American Welding Society, 2002.
[18] L. Zong, G. Shi, Y.Q. Wang, et al., Fatigue assessment on butt welded splices in plates of different thicknesses, Journal of Constructional Steel Research 129 (2017) 93–100.
[19] L. Zong, G. Shi, Y.Q. Wang, et al., Experimental and numerical investigation on fatigue performance of non-load-carrying fillet welded joints, Journal of Constructional Steel Research 130 (2017) 193–201.
[20] P. Paris, F. Erdogan, A critical analysis of crack propagation laws, Journal of Basic Engineering 85 (4) (1963) 528–534.
[21] K. Tanaka, Fatigue crack propagation from a crack inclined to the cyclic tensile axis, Engineering Fracture Mechanics 6 (3) (1974) 493–507.
[22] F. Erdogan, G.C. Sih, On the crack extension in plates under plane loading and transverse shear, Journal of Basic Engineering 85 (1963) 519–525.
[23] K. Palaniswamy, W.G. Knauss, Propagation of a crack under general, in-plane tension, International Journal of Fracture 8 (1) (1972) 114–117.
[24] G.C. Sih, Strain-energy-density factor applied to mixed mode crack problems, International Journal of Fracture 10 (1974) 305–321.
[25] Franc3D, Reference Manual for Version 6, Fracture Analysis Consultants Inc., 2011.
[28] British Standards Institution (BSI), BS 7910. Guide to Methods for Assessing the Acceptability of Flaws in Metallic Structures, BSI, London, 2005.
[29] J.B. Ibsø, H. Agerskov, An analytical model for fatigue life prediction based on fracture mechanics and crack closure, Journal of Constructional Steel Research 37 (3) (1996) 229–261.